

## Reactive extrusion and high-temperature oxidation of Ni<sub>3</sub>Al

K. MORSI\*

Department of Mechanical Engineering, San Diego State University, 5500, Campanile Drive, San Diego, California, 92182, USA

E-mail: kmorsi@mail.sdsu.edu

S. O. MOUSSA

Department of Chemistry, Ain Shams University, Cairo, Egypt

JAMES J. WALL

Department of Materials Science and Engineering, University of Tennessee, Knoxville, TN 37996, USA

**Published online:** 1 November 2005

The nickel aluminide (Ni<sub>3</sub>Al) intermetallic has attracted considerable attention over the past few decades due to its desirable properties at elevated temperatures [1]. A considerable amount of work has been reported on the combustion synthesis of nickel aluminides [2–7]. The process (in the thermal explosion mode of ignition) involves uniformly heating an elemental powder compact of nickel and aluminum to an ignition temperature (at or above the eutectic temperature of 640 °C) at which the reactant powder spontaneously convert to product(s). A general problem however is the generation of unwanted porosity in the final product, which necessitates the application of pressure (hot pressing/hot isostatic pressing) in order to produce highly dense materials [3, 4]. The current approach involves heating the compact to the ignition temperature, and allowing the exothermic reaction to proceed to completion inside the extrusion chamber, thereby raising the compact temperature to the maximum “combustion” temperature. Extrusion is then conducted as the specimen cools down from the combustion temperature. This reactive extrusion (RE) approach offers a number of possible advantages including, the production of completely reacted single phase alloys, consolidation, and grain size refinement through re-crystallization. Recent preliminary work by the authors showed the feasibility of the approach to produce Ni<sub>3</sub>Al [8]. Away from the die exit, the reactively extruded material was found to have a refined grain structure with an average grain size that increases from 4 to 6.5 μm along the extrusion length. In this paper, the effect of extrusion speed on the product microstructure and properties is discussed, together with a preliminary evaluation of the high-temperature oxidation behavior of reactively extruded Ni<sub>3</sub>Al and a comparison to that of combustion synthesized materials. *SHS* (self-propagating high temperature synthesis) extrusion of TiC reinforced with a metallic binder (e.g., Ni) (to facilitate

high-temperature deformation) was previously reported [9, 10]. This approach uses local ignition of the compact which sets off a self-sustaining exothermic reaction wave that travels along the specimen converting reactants to products. In the present study, nickel aluminide intermetallics (Ni<sub>3</sub>Al) were reactively extruded using the *thermal explosion* mode of ignition and therefore the material is more uniformly heated to the ignition temperature promoting a more uniform temperature distribution prior to extrusion (Fig. 1).

Elemental powders of gas-atomized aluminum (–325 mesh, 99.99% pure from Atlantic Equipment Engineers, NJ, USA), and nickel (3–7 μm particle size, 99.99% pure, INCO123 from INCO Selective Surfaces Inc., NJ, USA) were turbula mixed together with 10 vol.% pre-alloyed Ni<sub>3</sub>Al powders (–325 mesh, 99.0% pure, from Alfa Aesar, MA, USA). All powders were isostatically pressed to ~78% of the theoretical green density and then vacuum degassed at 300 °C for 12 hr. The compacts were then heated inside the extrusion chamber (15 mm inner diameter) maintained at a temperature of ~700 °C (with the aid of a knuckle heater). A combination of glass and graphite was used for lubrication. The compact temperature was monitored and recorded using a K-type thermocouple inserted into the bottom of the specimen through the die exit, which was then simply pushed out during extrusion. The extrusion stroke was initiated at 1000 °C and different speeds (6, 10, and 14 mm/s) while the specimen was cooling down from the combustion temperature. A conical die (semi-die angle α=32.5°) and extrusion ratio (area reduction) of 10:1 was used.

Following extrusion, the samples were ground to half thickness along the extrusion axis, then polished and etched for microstructural examination. Etching was carried out using an etchant of composition 60 vol.% distilled H<sub>2</sub>O, 20 vol.% HCl and 20 vol.% HNO<sub>3</sub>, and the aver-

\* Author to whom all correspondence should be addressed.

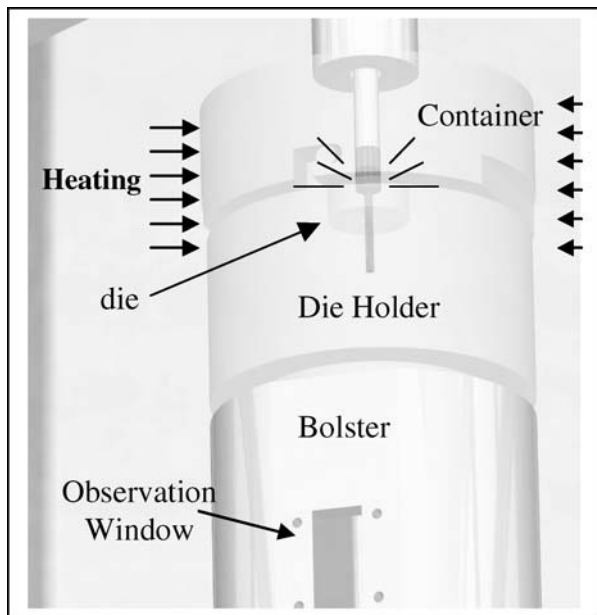


Figure 1 3D model of reactive extrusion setup.

age grain size was determined using the areal method according to ASTM standard [11]. The microstructure images were taken from exactly the mid point along the length of the extrusion for all extrudates using an optical microscope connected to a digital imaging processor (Image analysis, BUEHLER LTD., USA). Rockwell hardness measurements were also made on the same regions. For the high-temperature oxidation studies, the specimens of as-reactively processed  $\text{Ni}_3\text{Al}$  (reactively extruded (RE) and specimens that were reacted inside the container without extrusion, i.e., just combustion synthesized (CS) were cut into small rectangular sections (average initial weight of  $1.130 \pm 0.01$  g and cross sectional area of  $1.65 \pm 0.15$   $\text{cm}^2$ ). Prior to exposure, the specimens were ultrasonically cleaned, polished, and degreased in acetone, then placed in the furnace at  $1000$   $^\circ\text{C}$ . The specimens underwent hot corrosion in air ( $P_{\text{O}_2} \sim 0.2$  atm). All corrosion tests were cyclic tests; one cycle represents 40 hr exposure at the corrosion temperature, followed by

cooling to room temperature. After each cycle the mass change in the specimens was determined by weighing. Each value represents the average of three specimens with the scattered error being less than 16%. The entire exposure time at  $1000$   $^\circ\text{C}$  was 400 hr (10 cycles). Weight gain due to oxide scale formation at a given exposure time  $t$  (hr) was then plotted against exposure time for both the reactively extruded (initiated at  $1000$   $^\circ\text{C}$  and extrusion speed of 6 mm/s) and combustion synthesized specimens.

Following reactive extrusion, X-ray diffraction scans on the extruded product confirmed the formation of  $\text{Ni}_3\text{Al}$  (Fig. 2). For materials extruded at 14 mm/s, some trace of nickel oxide was observed.

Fig. 3 shows the effect of extrusion speed on the developed microstructure, grain size and hardness of the reactively processed materials. Compared to the combustion-synthesized material (CS- $\text{Ni}_3\text{Al}$ ), the reactively extruded specimens produced extrudates with consolidated microstructures and refined re-crystallized grains. Both pore elimination and a decrease in grain size had the effect of increasing the Rockwell hardness from  $53(\pm 3)$  HRA to greater than  $69(\pm 5)$  HRA.

The average grain size increases (with a resulting decrease in hardness) from RE specimens extruded at 6 mm/s to those extruded at strain rates of 14 mm/s. These results can be explained when we consider the processing conditions. Although extrusion in all specimens was initiated at a temperature of  $1000$   $^\circ\text{C}$ , before the actual extrusion is performed, the specimens would be first upset inside the extrusion container followed by some consolidation and pore closure. Although some compact self heating will occur due to work done by the ram, at the point of the actual extrusion, the specimens extruded at slower speeds would have cooled down more than those extruded at the higher speeds. Fig. 4 shows a plot of specimen temperature values taken at the point of actual material extrusion (i.e., corresponding to the peak extrusion pressure) versus the extrusion speeds used.

Grain growth is therefore more evident at those specimens extruded at the higher speeds with correspondingly higher extrusion temperatures.

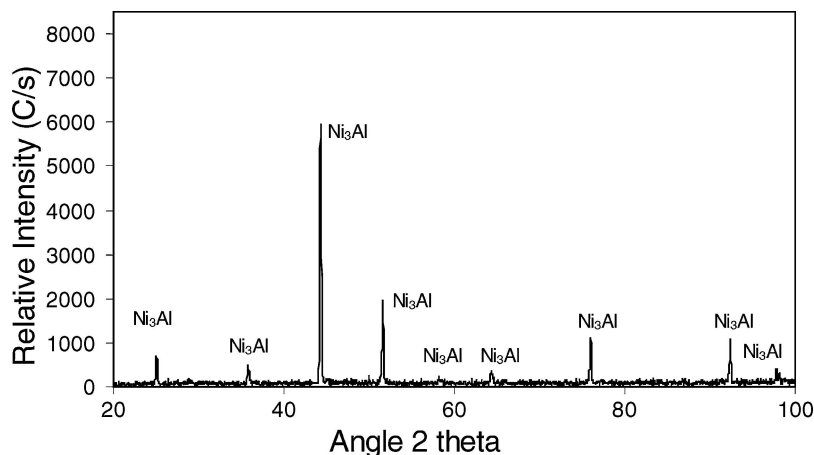


Figure 2 X-ray diffraction pattern for RE- $\text{Ni}_3\text{Al}$  (extrusion speed 6 mm/s).

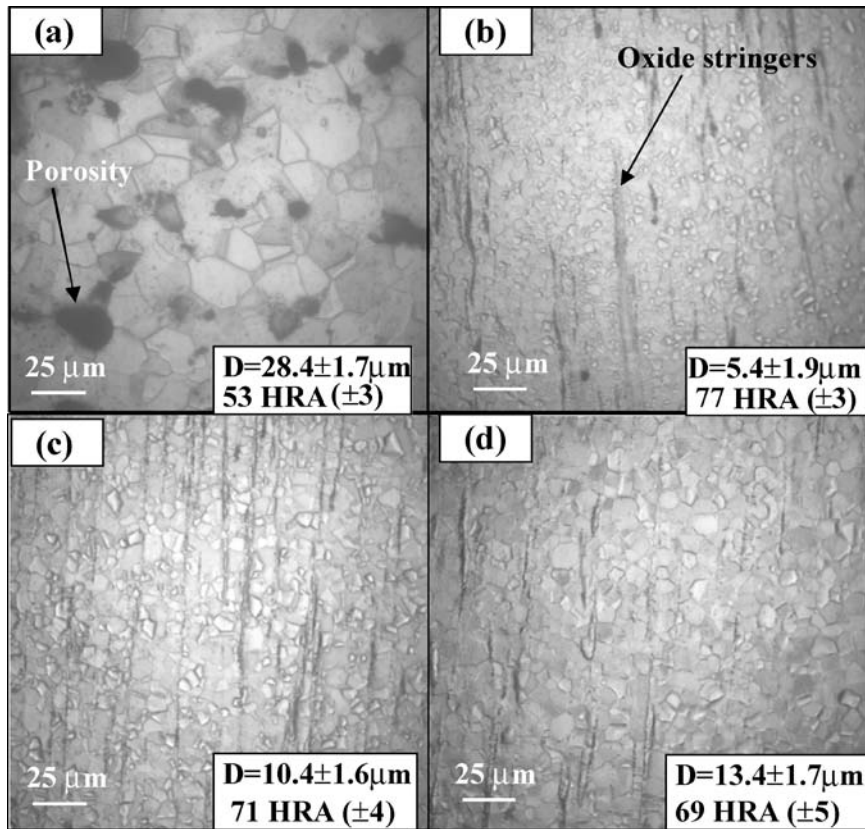


Figure 3 Micrographs showing effect of extrusion/extrusion speed on the developed microstructure, average grain size (D) and Rockwell hardness (HRA) of reactively extruded Ni<sub>3</sub>Al (a) reacted inside extrusion chamber but not extruded, (b) RE at extrusion speed of 6 mm/s, (c) RE at extrusion speed 10 mm/s, (d) RE at extrusion speed 14 mm/s.

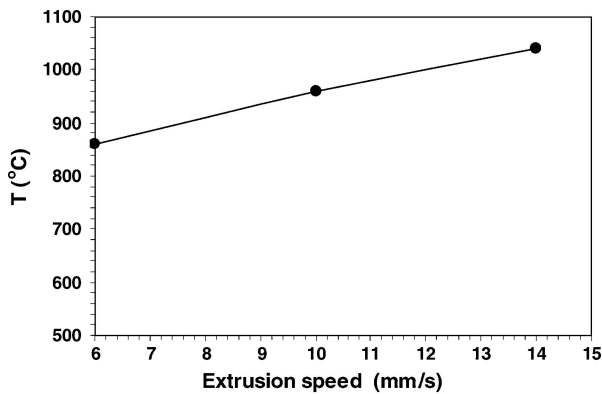


Figure 4 Temperature at the point of extrusion versus extrusion speed.

The micrographs of extruded specimens also show oxide stringers (presumably from oxides on the original powder) aligned in the direction of extrusion. All materials extruded were sound and in good condition except for the material extruded at 14 mm/s, in which the extrudate was fractured on extrusion. The time average mean strain rates ( $\dot{\epsilon}$ ) corresponding to the different extrusion speeds used were calculated from the extrusion ram speed ( $v$ ), extrusion ratio ( $R$ ) and container and extrusion diameters ( $D_b$  and  $D_e$ ) as follows [12]:

$$\dot{\epsilon} = \frac{6vD_b^2 \ln R \tan \alpha}{D_b^3 - D_e^3} \quad (1)$$

$\alpha$  is the semi die angle ( $\alpha=45^\circ$  in case of square die, and  $32.5^\circ$  for our conical dies). The 6, 10, and 14 mm/s speeds corresponded to 5.5, 9.1, and 12.8  $s^{-1}$ , respectively. Although the temperature at the point of extrusion is higher for the materials extruded at the higher speeds, the increased strain rates experienced by the material has led to a reduction in ductility, leading to fracture of the material on extrusion for the material extruded at 14 mm/s.

Fig. 5 shows that the weight gain per unit area ( $mg/cm^2$ ) due to the oxidation process of CS-Ni<sub>3</sub>Al is overwhelming compared to RE-Ni<sub>3</sub>Al (extrusion initiated at 1000 °C and

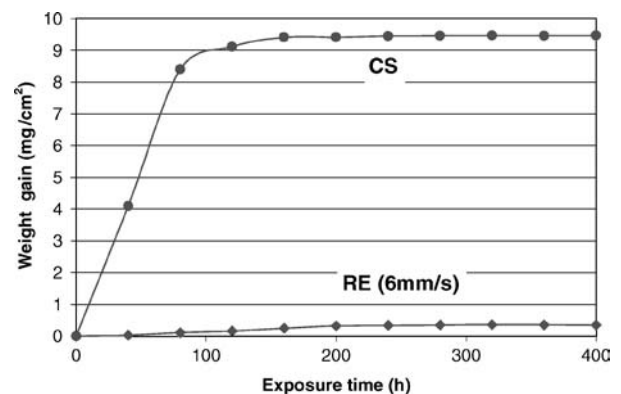


Figure 5 Weight gain per unit area during 400 hr cyclic exposure in oxygen atmosphere of as-processed Ni<sub>3</sub>Al.

extrusion speed 6 mm/s). This is believed to be a direct result of the porous microstructure of CS-Ni<sub>3</sub>Al in addition to its larger average grain size as described below. The higher the level of porosity, the more prone the material is to oxidation since pores will allow more oxygen into the material as well as increase its effective surface area. The oxide scale formed in CS-Ni<sub>3</sub>Al consisted of NiO (major phase) and NiAl<sub>2</sub>O<sub>4</sub> with a discontinuous internal layer of Al<sub>2</sub>O<sub>3</sub>. The starting grain size of the as-processed Ni<sub>3</sub>Al prior to the oxidation experiments also contributed significantly to the oxidation process. Recent work [13, 14] showed that nickel aluminides with small grain sizes (5–10 μm) oxidize less (i.e., small weight gain per unit area) than those with larger grains. This is due to small grains possessing high grain-boundary density, which act as easy-diffusion paths for Al atoms, resulting in a rapid formation of surface protective continuous inner layer of Al<sub>2</sub>O<sub>3</sub> and preventing further oxidation. Ni<sub>3</sub>Al produced via RE had a starting average grain size of ~5.5 μm prior to the oxidation process compared to ~28 μm produced via Combustion Synthesis. This therefore facilitated the production of a protective alumina layer for the RE specimens (experimentally confirmed by the authors, the details of which is the subject of a separate larger study). The results also further emphasize the importance of RE as a grain refining process (through re-crystallization). Future work should address detailed strategies; to identify the size of the processing window through which fully consolidated crack-free materials can be produced successfully, to model the process and to design high durability

tooling (since the temperature pressure and requirements can be demanding).

## References

1. V. K. SIKKA, J. T. MAVITY and K. ANDERSON, *Mater. Sci. Eng.* **A153** (1992) 712.
2. D. ALMAN and N. S. STOLOFF, *Int. J. Powd. Metall.* **27** (1991) 29.
3. W. MISLIOLEK and R. M. GERMAN, *Mater. Sci. Eng.* **A144** (1991) 1.
4. T. CHENG and J. SUN, *Scripta Metall. Mater.* **30** (1994) 247.
5. K. MORSI, H. B. MCSHANE and M. MCLEAN, *Metall. and Mater. Trans. A.* **31** (2000) 1663.
6. K. MORSI, H. B. MCSHANE and M. MCLEAN, *Mater. Sci. & Eng.* **A290** (2000) 39.
7. K. A. PHILPOT, Z. A. MUNIR and J. B. HOLT, *J. Mater. Sci.* **22** (1987) 159.
8. K. MORSI, S. O. MOUSSA and J. J. WALL, *ibid.* **40** (2005) 1027.
9. V. V. PODLESESOV, A. V. RADUGIN and A. M. STOLIN, A. G. MERZHANOV, Translated from Russian journal *Inzhenero-Fizicheskii Zhurnal (J. Eng. Phys. Thermophys.)*, **63** (1992) 525.
10. A. MERZHANOV, A. M. STOLIN and V. V. PODLESOV, *J. Europ. Ceram. Soc.* **17** (1997) 447.
11. Annual Book of ASTM Standards, "Metals-Mechanical Testing; Elevated and Low-Temperature Tests; Metallography" (ASTM 1916 Race street, Philadelphia, PA, USA, 1995) Vol. 3.01, p. 236.
12. G. E. DIETER, *Mechanical Metallurgy*, SI Metric Edition. (McGraw-Hill, London, 1988) p. 629.
13. P. PEREZ, J. L. GONZALES-CARRASCO and P. ADEVA, *Oxid. Met.* **49** (1998) 485.
14. *Idem. Corro. Sci.* **40** (1998) 631.

*Received 6 June  
and accepted 7 July 2005*